Non-invasive coronary angiography with multislice spiral computed tomography: impact of heart rate

K Nieman, B J Rensing, R-J M van Geuns, et al.

Heart 2002 88: 470-474
doi: 10.1136/heart.88.5.470

CARDIOVASCULAR MEDICINE

Non-invasive coronary angiography with multislice spiral computed tomography: impact of heart rate

K Nieman, B J Rensing, R-J M van Geuns, J Vos, P M T Pattynama, G P Krestin, P W Serruys, P J de Feyter

Heart 2002;**88**:470–474

See end of article for authors' affiliations

Correspondence to: Dr Koen Nieman, Thoraxcenter Bd 410, Erasmus University Medical Centre Rotterdam, PO Box 2040, Rotterdam 3000 CA, Netherlands; koennieman@hotmail.com

Accepted 4 July 2002

Objective: To evaluate the impact of heart rate on the diagnostic accuracy of coronary angiography by multislice spiral computed tomography (MSCT).
Design: Prospective observational study.
Patients: 78 patients who underwent both conventional and MSCT coronary angiography for suspicion of de novo coronary artery disease (n=53) or recurrent coronary artery disease after percutaneous intervention (n=25).
Setting: Tertiary referral centre.
Methods: Intravenously contrast enhanced MSCT coronary angiography was done during a single breath hold, and ECG synchronised images were reconstructed retrospectively. All coronary segments of ⩾ 2.0 mm without stents were evaluated by two investigators and compared with quantitative coronary angiography. Patients were classified according to the average heart rate (mean (SD)) into three equally sized groups: group 1, 55.8 (4.1) beats/min; group 2, 66.6 (2.8) beats/min; group 3, 81.7 (8.8) beats/min.
Results: Image quality was sufficient for analysis in 78% of the coronary segments in patients in group 1, 73% in group 2, and 54% in group 3 ($p < 0.01$). The sensitivity and specificity for detecting significant stenoses (⩾ 50% lumen reduction) in these assessable segments were: 97% (95% confidence interval (CI) 84% to 100%) and 96% in group 1; 74% (52% to 89%) and 94% in group 2; and 67% (33% to 90%) and 94% in group 3 ($p < 0.05$). Accounting for all segments of ⩾ 2.0 mm, including lesions in non-assessable segments as false negatives, the sensitivity decreased to 82% (28/34 lesions, 95% CI 69% to 91%), 61% (14/23 lesions, 42% to 77%), and 32% (6/19 lesions, 15% to 50%), respectively ($p < 0.01$).
Conclusions: MSCT allows reliable coronary angiography in patients with low heart rates.

Contrast enhanced multislice spiral computed tomography (MSCT) is a promising non-invasive technique for the detection, visualisation, and characterisation of stenotic coronary artery disease.[1–4] However, MSCT has relatively poor temporal resolution compared with other methods of non-invasive coronary imaging such as electron beam computed tomography (EBCT) and magnetic resonance imaging.[5–7] Therefore MSCT remains sensitive to cardiac motion artefacts.[1 2 8]

We investigated the impact of average heart rate during acquisition of the MSCT angiograms on the accuracy of the technique for detecting stenotic coronary artery disease.

METHODS

Population

MSCT angiography was undertaken in 78 patients (mean (SD) age 56.9 (10.1) years; 57 men, 21 women). They were suspected of having coronary artery disease (n = 53) or presented with recurrent symptoms after percutaneous coronary interventions (n = 25) (table 1). Exclusion criteria were: not being in sinus rhythm, having an allergy to iodine containing contrast media, renal failure (serum creatinine > 100 µmol/l), pregnancy, respiratory impairment, or pronounced cardiac failure.

The study was approved by the local ethics committee, and informed consent was obtained from all patients.

Data acquisition

Contrast enhanced MSCT examinations were done in the supine position during a single breath hold (Somatom Plus 4 VolumeZoom, Siemens AG, Forchheim, Germany). A fixed delay of 20 seconds was instituted between the start of the intravenous contrast injection (150 ml of Iomeprol (350 mgI/ml), given at a rate of 3.5–4.0 ml/s) and the onset of the scan. An ECG was recorded during the continuous CT data acquisition. A 4 × 1.0 mm scan protocol was applied at a table increment of 1.5 mm per gantry rotation (rotation time 500 ms) for heart rates of < 80 beats/min. At faster heart rates (⩾ 80 beats/min) the table feed could be increased to 2.0 mm per rotation. A tube voltage of 120 kV and a current of 300 mA were typically applied. Depending on the cardiac dimensions and table feed, the scan time varied between 25–45 seconds.

Image reconstruction

After acquisition of the raw spiral CT data, retrospective ECG synchronised slices were reconstructed. A detailed description of ECG gated image reconstruction can be found elsewhere.[9] In summary, a single slice can be reconstructed from the CT data from a 180° *x* ray tube rotation, acquired in 250 ms at a rotation time of 500 ms. When the heart rate is above 65 beats/min, data from consecutive cycles are combined, which improves the effective temporal resolution.

Depending on the instantaneous heart rate, the slice reconstruction time varies between 125–250 ms (fig 1). Because data were acquired continuously, the reconstruction window can be positioned at any point within the cardiac cycle.

Abbreviations: EBCT, electron beam computed tomography; MSCT; enhanced multislice spiral computed tomography

Table 1 Baseline characteristics, assessability, and diagnostic accuracy of multislice computed tomographic (MSCT) angiography in detecting ⩾ 50% coronary artery stenoses

		Groups			
		All (n=78)	Group 1 (n=26)	Group 2 (n=26)	Group 3 (n=26)
Baseline characteristics					
Heart rate (beats/min)	Mean (SD)	68.0 (12.1)	55.8 (4.1)	66.6 (2.8)	81.7 (8.8)
	Range	49 to 103	49 to 62	63 to 72	73 to 104
Age (mean (SD))		56.9 (10.1)	58.3 (9.7)	58.9 (9.7)	53.4 (10.2)
Sex (male/female)		57/21	18/8	23/3	16/10
⩾50% stenotic lesions*		57 (76)	29 (34)	19 (23)	9 (19)
Stents		31	9	15	7
Assessability					
Relevant segments†		741	244	251	246
Assessable segments‡		505 (68%)	191 (78%)	182 (73%)	132 (54%)
Causes of non-assessability‡	Cardiac motion	73 (10%)	10 (4%)	15 (6%)	48 (20%)
	Calcifications	40 (5%)	17 (7%)	15 (6%)	8 (3%)
	Other causes¶	35 (5%)	5 (2%)	4 (2%)	26 (11%)
	Non-specific	88 (12%)	21 (9%)	35 (14%)	32 (13%)
Diagnostic accuracy (95% CI)					
Assessable coronary segments	Sensitivity	84% (74% to 92%)	97% (84% to 100%)	74% (52% to 89%)	67% (33% to 90%)
	Specificity	95% (93% to 96%)	96% (94% to 97%)	94% (91% to 96%)	94% (91% to 95%)
	Positive predictive value	67% (58% to 73%)	82% (71% to 85%)	58% (41% to 70%)	43% (21% to 58%)
	Negative predictive value	98% (97% to 99%)	99% (97% to 100%)	97% (94% to 99%)	97% (95% to 99%)
Sensitivity including non-assessable segments (95% CI)§		63% (54% to 71%)	82% (69% to 91%)	61% (42% to 77%)	32% (15% to 50%)
Accuracy at patient level**		56%	73%	54%	42%
Causes of misinterpretation	Total misinterpretations	33	7	15	11
	Calcification	17	5	8	4
	Cardiac motion	11	–	5	6
	Other causes	5	2	2	1

*The number of lesions including non-assessable segments given in brackets.
†All ⩾2.0 mm segments, but excluding segments containing stents.
‡Percentages of the (relevant) ⩾2.0 mm segments given in brackets.
¶Other causes include: respiratory motion, blending with adjacent contrast filled structures (vein, right ventricle), artefacts from pacemaker wire.
§Sensitivity including undetected lesions in non-assessable segments as false-negative.
**Percentage of patients with completely true positive or true negative diagnoses, including undetected lesions in non-assessable segments as false negative.
CI, confidence interval.

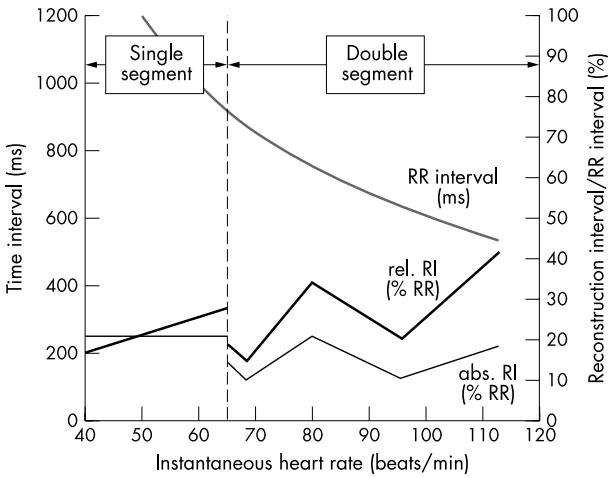

Figure 1 Heart rate dependency of the temporal resolution. Isocardiophasic transverse slices are reconstructed according to the recorded ECG using a 180° rotation partial scan algorithm. For heart rates up to 65 beats/min a single segment reconstruction algorithm is applied to reconstruct slices during a 250 ms reconstruction window (abs. RI) within each separate cardiac cycle. To improve the effective temporal resolution and reduce motion artefacts, a double segment reconstruction algorithm—which combines isocardiophasic data from two consecutive RR intervals—is applied at heart rates over 65 beats/min. The effective reconstruction interval per cardiac cycle depends on a complex relation between the gantry rotation time and the duration of the cardiac cycle. At a given rotation speed it varies between 125 ms at favourable and 250 ms at unfavourable heart rates. The relative reconstruction interval (rel. RI)—that is, the ratio between the absolute reconstruction interval and the total R to R wave interval (%)—progressively increases at higher heart rates (Siemens Somatom Plus 4 VolumeZoom with a rotation time of 500 ms).

Routinely, at least three datasets with reconstruction windows starting at 300 ms, 400 ms, and 500 ms before the onset of the next R wave were reconstructed. Other window positions within the diastolic phase were reconstructed if no satisfactory result was achieved. In a side by side comparison of the axial slices, the dataset with least motion artefacts was then selected for further analysis.

Typically a dataset at around 400 ms reconstruction showed the best result, but at higher heart rates the most optimal window was positioned closer towards 300 ms before the next R wave. Besides retrospective ECG gating, spiral scanning also allows selection of an image reconstruction increment (0.5 mm) below the effective slice thickness (1.25 mm). As a result of the overlapping slice reconstruction, near-isotropic voxel dimensions are created ($0.3 \times 0.3 \times 0.5$ mm).

Image processing

The image datasets were processed on a separate workstation and analysed using multiplanar reconstruction, thin slab maximum intensity projections, and volume rendering, in addition to the axial source images. Blinded for the conventional coronary angiography findings, two investigators assessed each coronary artery segment (according to the American Heart Association guidelines) and a final decision

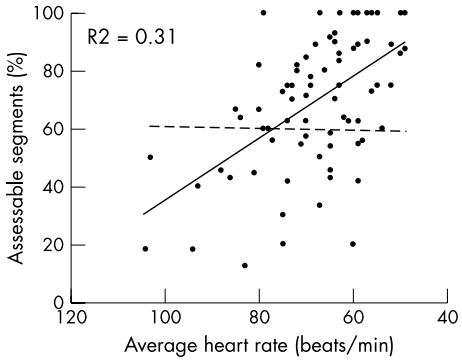

Figure 2 Heart rate dependency of coronary segment assessability. At lower heart rates ⩾ 2.0 mm segments per patient are assessable. The interrupted trend line represents the number of segments of ⩾ 2.0 mm diameter, as a ratio of 16 potentially available segments, which is independent of the patient's heart rate.

was reached by consensus.[10] Depending on the image quality, each vessel segment was classified as either assessable or not. Because of metal artefacts, coronary segments containing stents were excluded from assessment. Vessel segments with a diameter of ⩾ 2.0 mm, according to quantitative coronary angiography, were screened for the presence of ⩾ 50% lumen diameter reduction and compared with the results of the conventional angiographic examination.

Statistical analysis

Continuous variables are expressed as mean (SD). Descriptive statistics, sensitivity, specificity, negative predictive value, and positive predictive value, using a 95% confidence interval (CI), were stratified according to average heart rate in three equally sized groups. A χ^2 test was used to compare dichotomous variables. The diagnostic value was given for assessable segments, all segments of ⩾ 2.0 mm, and per patient. For analyses that include both assessable and non-assessable segments, the undetected lesions were classified as false negative results. Conventional (quantitative) coronary angiography was regarded as the gold standard.

RESULTS

The mean (SD) data acquisition time was 36.9 (3.8) seconds. Overall, 505 (68%) of 741 coronary segments could be assessed. In patients with a lower average heart rate, more segments of ⩾ 2.0 mm were assessable (fig 2). In all, 48 of 57 significant stenoses (84%) and 424 of 448 normal and non-significantly narrowed segments (98%) were correctly identified in the assessable segments (fig 3). The positive and negative predictive value were 67% and 98%, respectively. Including stenotic lesions in non-assessable segments, the overall sensitivity decreased to 64% (48 of 76 lesions). Misinterpretations, both false positive and negative, were caused by calcification and motion artefacts.

The total group of 78 patients was divided into three groups of 26 patients according to their heart rate ranking from low to high. The quality of the MSCT images of patients in group 1, with the lowest heart rate (mean (SD) 55.8 (4.1) beats/min, range 49–62), was sufficient for analysis in 78% of the coronary segments. For patients in group 2 (66.6 (2.8) beats/min, range 63–72) and group 3 (81.7 (8.8) beats/min, range 73–104), 73% and 54% of the segments, respectively, were assessable ($p < 0.01$). The sensitivity and specificity for detecting significant stenoses in the assessable segments were 97% (28/29) and 96%, 74% (14/19) and 94%, and 67% (6/9) and 94%, for groups 1, 2, and 3, respectively ($p < 0.05$). Accounting for all segments of ⩾ 2.0 mm, including lesions in non-assessable segments as false negatives, the sensitivity decreased to 82% (28/34), 61% (14/23), and 32% (6/19), respectively ($p < 0.01$).

Complete and accurate results were achieved more often in patients in group 1 (73%) than in those in group 2 (54%) or group 3 (42%). Only at high heart rates (group 3) were significantly more right coronary artery segments classified as non-assessable in comparison with left anterior descending coronary artery segments—58% and 35%, respectively ($p < 0.01$). These findings are amplified in table 1 and illustrated by representative cases in fig 4. The interobserver and intraobserver variability (the latter based on 19 randomly selected patients) for detecting stenosis were reasonably good, with κ values of 0.69 and 0.64, respectively.

From the recorded ECGs of 10 randomly selected patients we calculated the averaged relative heart rate variation during the scan. Initially, a brief deceleration can be observed; after approximately 20 seconds, however, the heart rate progressively increases (fig 5).

DISCUSSION

Residual cardiac motion artefacts remain a major cause of image degradation in MSCT coronary angiography.[2 3 8] The right coronary artery appears particularly vulnerable because of its extensive motion radius and short motion-free period.[11] In a recently published study, an inverse relation between heart rate

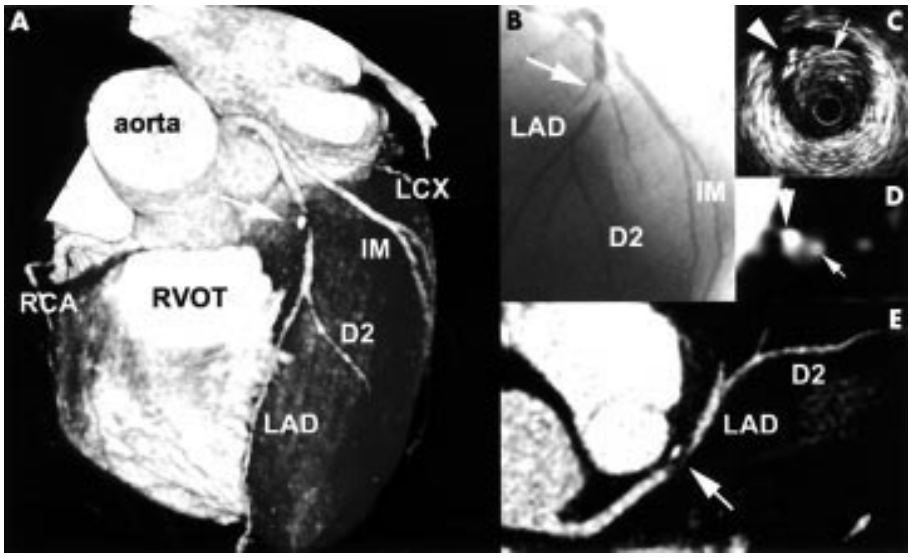

Figure 3 Multislice computed tomography (MSCT) angiogram of an obstructed left anterior coronary artery (LAD) and a heart rate of 49 beats/min. A significant stenosis (arrow) can be observed in the LAD. The three dimensional volume rendered overview (A) shows the lesion just distal to a small diagonal branch, which is confirmed by conventional angiography (B). The cross sectional (D) and longitudinal reconstructions (E) show a partially calcified lesion, which is confirmed by intracoronary ultrasound (C). D2, second diagonal branch; IM, intermediate branch; LCX, left circumflex coronary artery; RCA, right coronary artery. RVOT, right ventricular outflow tract

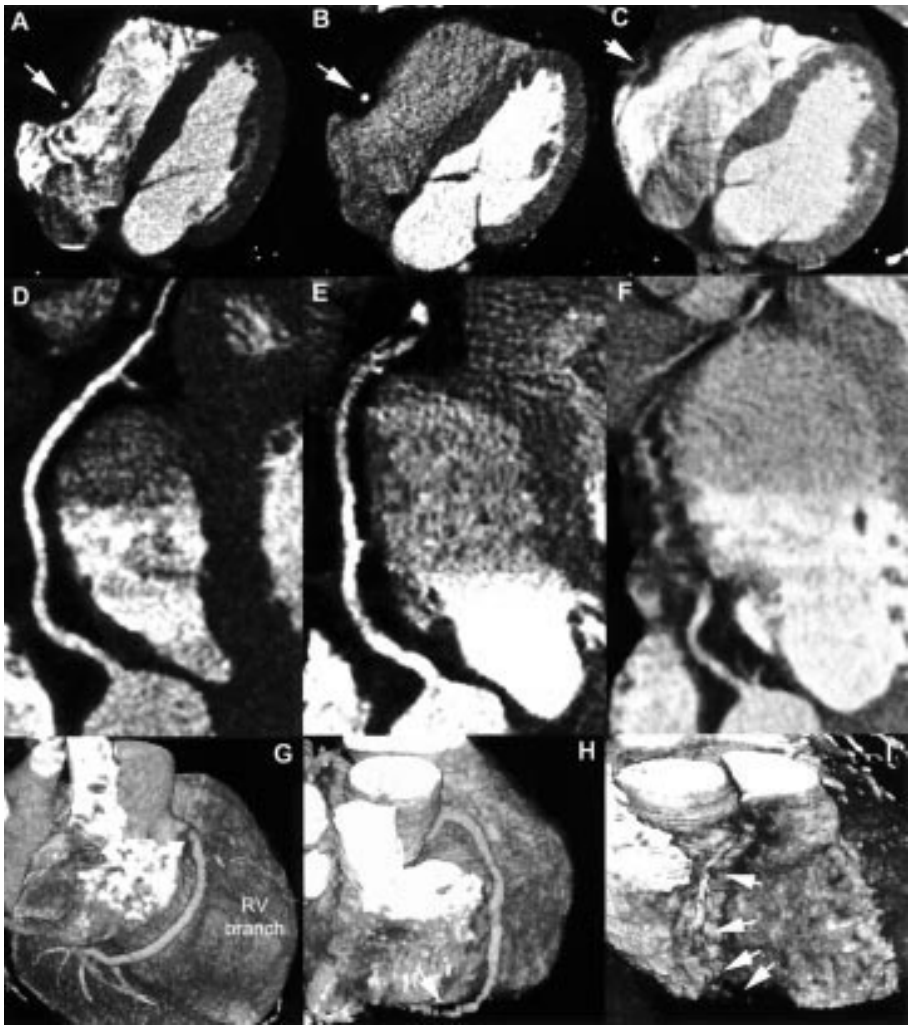

Figure 4 Multislice computed tomography (MSCT) angiograms at different heart rates. The axial source images (A,B,C), curved multiplanar reconstructions (D,E,F), and volume rendered reconstructions (G,H,I) of a normal right coronary artery (RCA, arrows) in patients with an average heart rate of 49 beats/min (A,D,G), 64 beats/min (B,E,H), and 81 beats/min (C,F,I), respectively, are shown. Motion artefacts (arrowheads) hinder assessment of the distal RCA in the second case and nearly the entire RCA in the third. RV, right ventricle.

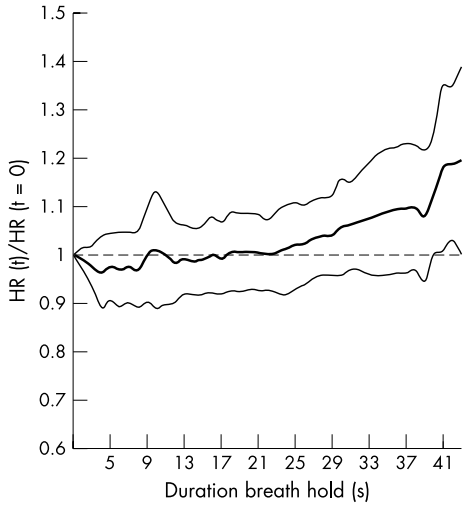

Figure 5 Heart rate variation during breath holding. Averaged relative heart rate (SD) of 10 randomly selected cases is shown. After an initial deceleration caused by a Valsalva induced vagal response, the heart rate progressively increases after approximately 20 seconds.

and the image quality of MSCT coronary angiography was reported.[12] However, that study did not investigate the consequences for diagnostic accuracy because there was no comparison with a gold standard (conventional angiography).

MSCT image reconstruction takes place during the diastolic phase when motion is relatively sparse.[11] The length of this motion-free period is inversely related to the heart rate. Conversely, there is a direct relation between the length of the reconstruction interval—that is, the temporal resolution—and the occurrence of cardiac motion artefacts. The temporal resolution depends on the gantry rotation time, which, owing to mechanical constraints, is currently limited to a maximum of 500 ms. Thus, by using a standard 180° rotation reconstruction algorithm, the temporal resolution is 250 ms. For comparison, EBCT has a temporal resolution of 100 ms and most magnetic resonance coronary angiography sequences use acquisition windows of between 100–150 ms.[6 7] At low heart rates a sufficiently long motion-free window is usually available during the mid-diastolic phase. Because this window narrows at higher heart rates, an algorithm has been developed that combines data from consecutive heart cycles and thereby potentially reduces the reconstruction time per cycle down to 125 ms. Optimal performance with this bisegmental algorithm can only be achieved at certain favourable heart rates. Furthermore, this potential reduction of motion artefacts comes at the price of a higher radiation exposure because the algorithm requires a relatively low table speed.

Besides motion artefacts, other factors such as the presence of high density material (stents or coronary calcifications), adjacent contrast filled cavities and veins, and incomplete breath holding complicate the assessment of the coronary arteries. Extensive calcium deposition causes high density artefacts that prevent proper luminal assessment. In our

group with the lowest heart rates, calcifications were the most common cause of assessment limitation and lesion misinterpretation. Patients with advanced coronary atherosclerosis do not currently benefit from MSCT angiography, and non-enhanced computed tomography, which detects extensive calcium deposition, can be helpful in identifying these patients.

Despite the optimisation of the temporal resolution at higher heart rates, we have shown that the assessability and diagnostic accuracy are significantly higher at lower heart rates, and deteriorate at higher heart rates. A temporary reduction in heart rate by giving short acting oral or intravenous β receptor blocking agents before the data acquisition can be expected to improve image quality. A reduction in the total scan time, either by faster gantry rotation or by more slices, will reduce the heart rate acceleration towards the end of the breath hold. A short scan time will also be beneficial in respect of venous contrast enhancement and patient motion.

Authors' affiliations
K Nieman, B J Rensing, R-J M van Geuns, J Vos, P W Serruys, P J de Feyter, Thoraxcenter, Department of Cardiology, Erasmus University Medical Centre, Rotterdam, Netherlands
P M T Pattynama, G P Krestin, Department of Radiology, Erasmus University Medical Centre

REFERENCES

1 **Nieman K**, Oudkerk M, Rensing BJ, *et al*. Coronary angiography with multi-slice computed tomography. *Lancet* 2001;**357**:599–603.
2 **Achenbach S**, Giesler T, Ropers D, *et al*. Detection of coronary artery stenoses by contrast-enhanced, retrospectively electrocardiographically-gated, multislice spiral computed tomography. *Circulation* 2001;**103**:2535–8.
3 **Knez A**, Becker C, Leber A, *et al*. Non-invasive angiography with multi-detector helical computed tomography for evaluation of coronary artery disease [abstract]. *J Am Coll Cardiol* 2000;**101**(suppl A):463.
4 **Schroeder S**, Kopp AF, Baumbach A, *et al*. Noninvasive detection and evaluation of atherosclerotic coronary plaques with multislice computed tomography. *J Am Coll Cardiol* 2001;**37**:1430–5.
5 **Ohnesorge B**, Flohr T, Becker C, *et al*. Cardiac imaging by means of electrocardiographically gated multisection spiral CT: initial experience. *Radiology* 2000;**217**:564–71.
6 **Wielopolski PA**, van Geuns RJ, de Feyter PJ, *et al*. Coronary arteries. *Eur Radiol* 2000;**10**:12–35.
7 **Rensing BJ**, Bongaerts A, van Geuns RJ, *et al*. Intravenous coronary angiography by electron beam computed tomography: a clinical evaluation. *Circulation*. 1998;**98**:2509–12.
8 **Achenbach S**, Ulzheimer S, Baum U, *et al*. Noninvasive coronary angiography by retrospectively ECG-gated multislice CT. *Circulation* 2000;**102**:2823–8.
9 **Ohnesorge B**, Flohr T, Becker C, *et al*. Technical aspects and applications of fast multislice cardiac CT. In: Reiser MF, Takahashi M, Modic M, *et al*, eds. *Medical radiology – diagnostic imaging and radiation oncology*. Berlin: Springer, 2001:121–30.
10 **Austen WG**, Edwards JE, Frye RL, *et al*. A reporting system on patients evaluated for coronary artery disease. Report of the ad hoc committee for grading of coronary artery disease, Council on Cardiovascular Surgery, American Heart Association. *Circulation* 1975;**51**:5–40.
11 **Wang Y**, Vidan E, Bergman GW. Cardiac motion of coronary arteries: variability in the rest period and implications for coronary MR angiography. *Radiology* 1999;**213**:751–8.
12 **Hong C**, Becker CR, Huber A. ECG-gated reconstructed multi-detector row CT coronary angiography: effect of varying trigger delay on image quality. *Radiology* 2001;**220**:712–17.

IMAGES IN CARDIOLOGY

Large thrombus entrapped in a patent foramen ovale of the atrial septum, which apparently "disappeared" without embolic events

A 59 year old woman, 12 days after haematoma evacuation for hypertensive right putaminal haemorrhage, suddenly complained of dyspnoea and then collapsed just after she had started to walk. She was admitted to our hospital after cardiopulmonary resuscitation. On admission, the patient was in stable haemodynamic condition. She had a left hemiparesis and was slightly dyspnoeic, and had a Glasgow coma score of 15. Transthoracic echocardiography revealed right ventricular dilatation and floating structures in the right atrium, but the interatrial septum could not be clearly seen. Transoesophageal echocardiography revealed a large, snake-like structure crossing the foramen ovale of her interatrial septum. Each part of the structure in the right and left atrium was floating (top left panel: LA, left atrium: RA, right atrium). Unfortunately, despite the urgency of the situation, anticoagulation treatment or surgical removal of the thrombus could not be performed because of the patient's recent cerebral haemorrhage. She was scheduled for surgery 10 days after admission (22 days after the cerebral haematoma evacuation).

The patient showed no clinical signs following the pulmonary embolism or paradoxical systemic embolism in the days preceding the operation. On the day of planned surgery, transoesophageal echocardiography revealed no thrombi in any cardiac chambers (top right panel). Atrial–atrial shunt could not be detected by using colour Doppler echocardiography. Contrast right-to-left shunting was detected immediately after the right atrial opacification phase (bottom panel: A, precontrast injection; B and C, contrast right-to-left shunting was detected immediately after the right atrial opacification phase; SVC, superior vena cava). Clinically, there was no evidence of thromboembolism. The patient was discharged after implantation of an inferior vena cava filter and is doing well without additional embolic events.

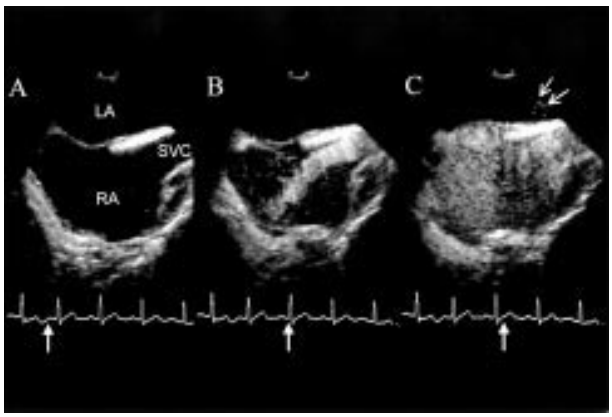

N Watanabe
T Akasaka
K Yoshida
non@med.kawasaki-m.ac.jp